

Avoiding entanglement sudden death using single-qubit quantum measurement reversal

Hyang-Tag Lim,^{1,2} Jong-Chan Lee,¹ Kang-Hee Hong,¹
and Yoon-Ho Kim^{1,*}

¹*Department of Physics, Pohang University of Science and Technology (POSTECH), Pohang,
790-784, South Korea*

²*forestht@gmail.com*

**yoanho72@gmail.com*

<http://qopt.postech.ac.kr>

Abstract: When two entangled qubits, each owned by Alice and Bob, undergo separate decoherence, the amount of entanglement is reduced, and often, weak decoherence causes complete loss of entanglement, known as entanglement sudden death. Here we show that it is possible to apply quantum measurement reversal on a single-qubit to avoid entanglement sudden death, rather than on both qubits. Our scheme has important applications in quantum information processing protocols based on distributed or stored entangled qubits as they are subject to decoherence.

© 2014 Optical Society of America

OCIS codes: (270.5585) Quantum information and processing; (270.5565) Quantum communications.

References and links

1. M. A. Nielsen and I. L. Chuang, *Quantum Computation and Quantum Information* (Cambridge University, Cambridge, 2000).
2. C. H. Bennett and D. P. DiVincenzo, "Quantum information and computation," *Nature (London)* **404**, 247–255 (2000).
3. C. H. Bennett, G. Brassard, C. Crépeau, R. Jozsa, A. Peres, and W. K. Wootters, "Teleporting an unknown quantum state via dual classical and Einstein-Podolsky-Rosen channels," *Phys. Rev. Lett.* **70**, 1895–1899 (1993).
4. D. Bouwmeester, J.-W. Pan, K. Mattle, M. Eibl, H. Weinfurter, and A. Zeilinger, "Experimental quantum teleportation," *Nature (London)* **390**, 575–579 (1997).
5. N. Gisin, G. Ribordy, W. Tittel, and H. Zbinden, "Quantum cryptography," *Rev. Mod. Phys.* **74**, 145–195 (2002).
6. T. Yu and J. H. Eberly, "Finite-time disentanglement via spontaneous emission," *Phys. Rev. Lett.* **93**, 140404 (2004).
7. M. P. Almeida, F. de Melo, M. Hor-Meyll, A. Salles, S. P. Walborn, P. H. Souto Ribeiro, and L. Davidovich, "Environment-induced sudden death of entanglement," *Science* **316**, 579–582 (2007).
8. D. A. Lidar, I. L. Chuang, and K. B. Whaley, "Decoherence-free subspaces for quantum computation," *Phys. Rev. Lett.* **81**, 2594–2597 (1998).
9. P. G. Kwiat, A. J. Berglund, J. B. Altepeter, and A. G. White, "Experimental verification of decoherence-free subspaces," *Science* **290**, 498–501 (2000).
10. P. Facchi, D. A. Lidar, and S. Pascazio, "Unification of dynamical decoupling and the quantum Zeno effect," *Phys. Rev. A* **69**, 032314 (2004).
11. S. Maniscalco, F. Francica, R. L. Zaffino, N. L. Gullo, and F. Plastina, "Protecting entanglement via the quantum Zeno effect," *Phys. Rev. Lett.* **100**, 090503 (2008).
12. J. G. Oliveira, Jr., R. Rossi, Jr., and M. C. Nemes, "Protecting, enhancing, and reviving entanglement," *Phys. Rev. A* **78**, 044301 (2008).

13. J. A. Schreier, A. A. Houck, Jens Koch, D. I. Schuster, B. R. Johnson, J. M. Chow, J. M. Gambetta, J. Majer, L. Frunzio, M. H. Devoret, S. M. Girvin, and R. J. Schoelkopf, "Suppressing charge noise decoherence in superconducting charge qubits," *Phys. Rev. B* **77**, 180502(R) (2008).
14. L. Viola, E. M. Fortunato, M. A. Pravia, E. Knill, R. Laflamme, and D. G. Cory, "Experimental realization of noiseless subsystems for quantum information processing," *Science* **293**, 2059–2063 (2001).
15. D. Kielpinski, V. Meyer, M. A. Rowe, C. A. Sackett, W. M. Itano, C. Monroe, and D. J. Wineland, "A decoherence-free quantum memory using trapped ions," *Science* **291**, 1013–1015 (2001).
16. M. Koashi and M. Ueda, "Reversing measurement and probabilistic quantum Error correction," *Phys. Rev. Lett.* **82**, 2598–2601 (1999).
17. A. N. Korotkov and A. N. Jordan, "Undoing weak quantum measurement of a solid-state qubit," *Phys. Rev. Lett.* **97**, 166805 (2006).
18. Q. Sun, M. Al-Amri, and M. S. Zubairy, "Reversing the weak measurement of an arbitrary field with finite photon number," *Phys. Rev. A* **80**, 033838 (2009).
19. N. Katz, M. Neeley, M. Ansmann, R. C. Bialczak, M. Hofheinz, E. Lucero, A. O'Connell, H. Wang, A. N. Cleland, J. M. Martinis, and A. N. Korotkov, "Reversal of the weak measurement of a quantum state in a superconducting phase qubit," *Phys. Rev. Lett.* **101**, 200401 (2008).
20. Y.-S. Kim, Y.-W. Cho, Y.-S. Ra, and Y.-H. Kim, "Reversing the weak quantum measurement for a photonic qubit," *Opt. Express* **17**, 11978–11985 (2009).
21. A. N. Korotkov and K. Keane, "Decoherence suppression by quantum measurement reversal," *Phys. Rev. A* **81**, 040103(R) (2010).
22. J.-C. Lee, Y.-C. Jeong, Y.-S. Kim, and Y.-H. Kim, "Experimental demonstration of decoherence suppression via quantum measurement reversal," *Opt. Express* **19**, 16309–16316 (2011).
23. Q. Sun, M. Al-Amri, L. Davidovich, and M. S. Zubairy, "Reversing entanglement change by a weak measurement," *Phys. Rev. A* **82**, 052323 (2010).
24. Y.-S. Kim, J.-C. Lee, O. Kwon, and Y.-H. Kim, "Protecting entanglement from decoherence using weak measurement and quantum measurement reversal," *Nature Phys.* **8**, 117–120 (2012).
25. C. H. Bennett, H. J. Bernstein, S. Popescu, and B. Schumacher, "Concentrating partial entanglement by local operations," *Phys. Rev. A* **53**, 2046–2052 (1996).
26. C. H. Bennett, G. Brassard, S. Popescu, B. Schumacher, J. A. Smolin, and W. K. Wootters, "Purification of noisy entanglement and faithful teleportation via noisy channels," *Phys. Rev. Lett.* **76**, 722–725 (1996).
27. P. G. Kwiat, S. Barraza-Lopez, A. Stefanov, and N. Gisin, "Experimental entanglement distillation and 'hidden' non-locality," *Nature (London)* **409**, 1014–1017 (2001).
28. J.-W. Pan, C. Simon, Č. Brukner, and A. Zeilinger, "Entanglement purification for quantum communication," *Nature (London)* **410**, 1067–1070 (2001).
29. J. P. Groen, D. Ristè, L. Tornberg, J. Cramer, P. C. de Groot, T. Picot, G. Johansson, and L. DiCarlo, "Partial-measurement backaction and nonclassical weak values in a superconducting circuit," *Phys. Rev. Lett.* **111**, 090506 (2013).
30. W. K. Wootters, "Entanglement of formation of an arbitrary state of two qubits," *Phys. Rev. Lett.* **80**, 2245–2248 (1998).
31. Y. H. Shih and C. O. Alley, "New type of Einstein-Podolsky-Rosen-Bohm experiment using pairs of light quanta produced by optical parametric down conversion," *Phys. Rev. Lett.* **61**, 2921–2924 (1988).

1. Introduction

Quantum entanglement is an essential resource for quantum information processing including quantum computation [1, 2] and quantum communication [3–5]. However, decoherence due to irreversible interactions with the environment causes degradation of entanglement, and, in some cases, leads to entanglement sudden death (ESD) in which entanglement is completely lost before its subsystem is fully decohered [6, 7]. Since overcoming decoherence is required for practical realization of quantum information protocols, various schemes for suppressing decoherence have been reported [8–15].

Recently, it has been shown that quantum measurement reversal, a set of weak and reversing measurements [16–20], can effectively suppress decoherence [21–24]. Without quantum measurement reversal, decoherence causes the qubit to end-up in a mixed state due to the loss of quantum coherence, while if quantum measurement reversal is introduced as shown in Fig. 1(a), the initial state may be preserved even in the presence of decoherence [21, 22]. This decoherence suppression scheme can also be applied to multi-qubit systems, in particular, it has been shown that entanglement of two-qubit states that undergo separate decoherence can be protected by

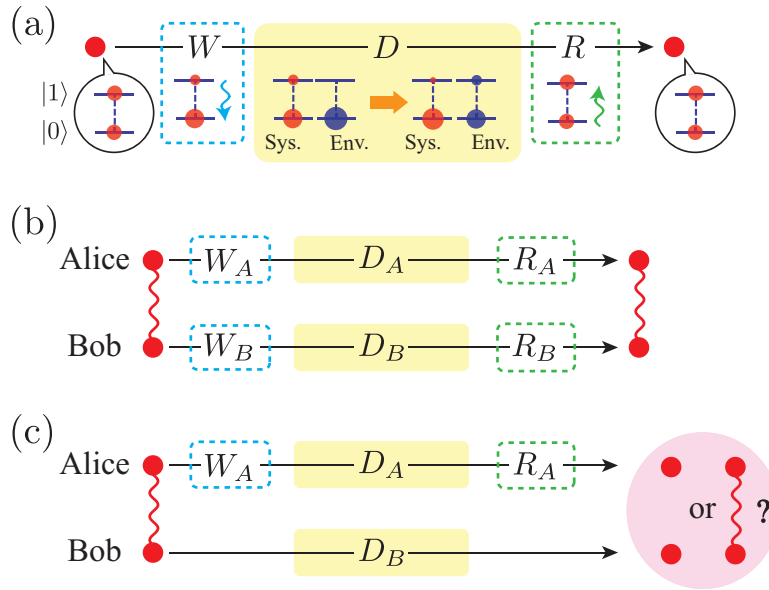


Fig. 1. (a) Decoherence suppression scheme using quantum measurement reversal for a single qubit state. To suppress decoherence, a set of weak and reversing measurements are performed before and after decoherence, respectively. Note that the size of the spheres corresponds to the population fraction of each level, $|0\rangle$ and $|1\rangle$. (b) Entanglement of two-qubit states which undergo separate decoherence can be recovered if both Alice and Bob carry out quantum measurement reversal. (c) The situation we considered here: Only Alice performs single-qubit quantum measurement reversal on her subsystem. W : weak measurement, D : decoherence, R : reversing measurement, Sys: system, Env: environment.

using two sets of single-qubit quantum measurement reversal steps, see Fig. 1(b) [24]. In some cases, decoherence affecting on both subsystems of two-qubit entangled states causes complete loss of entanglement, i.e., ESD [6]. Interestingly, even in this severe circumstance, the initial entanglement can be protected by performing quantum measurement reversal on both qubits. Avoiding ESD is essential in entanglement distribution between two distant parties, since once distributed entangled qubits completely lose entanglement, entanglement cannot be distilled between them [25–28].

A question then naturally arises whether preventing an entangled state from completely losing entanglement against ESD is possible by quantum measurement reversal performed only on one of the qubits rather than on both qubits as shown in Fig. 1(c). For instance, between Alice and Bob who initially share two entangled qubits, only Alice performs quantum measurement reversal on her qubit. In this work, we demonstrate that Alice alone can avoid ESD by performing quantum measurement reversal only on her qubit.

2. Theory

Consider the situation in which a two-qubit entangled state is affected by separate decoherence. Initially, Alice and Bob share two-qubit pure entangled state $|\Phi\rangle = \alpha|00\rangle + \beta|11\rangle$ where $|\alpha|^2 + |\beta|^2 = 1$ as shown in Fig. 2(a). We assume that each qubit independently suffers from amplitude damping decoherence. In general, amplitude damping decoherence arises due to the interaction between the system (S) and the environment (E) and amplitude damping for a single qubit can be represented by the following operation, $|0\rangle_S|0\rangle_E \rightarrow |0\rangle_S|0\rangle_E$ and $|1\rangle_S|0\rangle_E \rightarrow \sqrt{D}|1\rangle_S|0\rangle_E +$

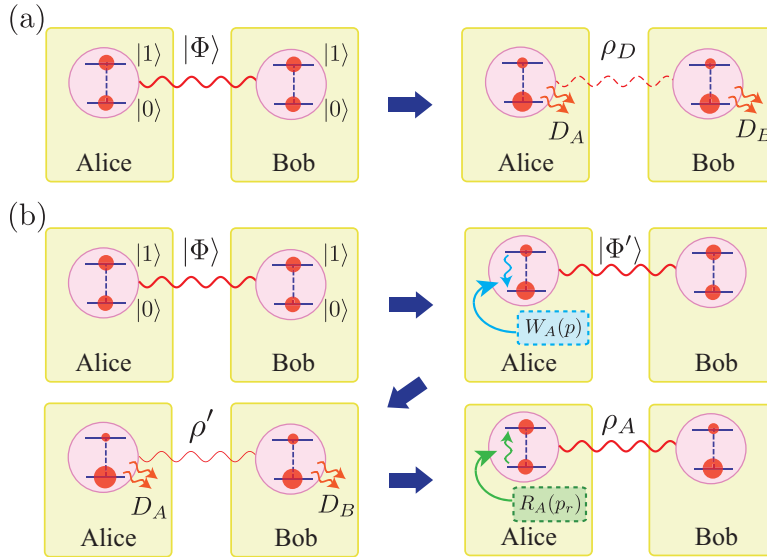


Fig. 2. (a) Alice and Bob initially share a pure entangled state $|\Phi\rangle$. When both subsystems suffer from decoherence, the final state ρ_D loses its entanglement partially or completely. (b) To suppress decoherence, Alice performs a set of weak measurement $W_A(p)$ and reversing measurement $R_A(p_r)$ before and after her subsystem undergoes decoherence, respectively. Then, the resulting state ρ_A becomes closer to the initial state $|\Phi\rangle$, i.e. ρ_A is more entangled than ρ_D . Note that Bob is not involved in this decoherence suppression scheme.

$\sqrt{D}|0\rangle_S|1\rangle_E$, where $0 \leq D \leq 1$ is the magnitude of the decoherence and $\bar{D} \equiv 1 - D$. Amplitude damping usually describes the energy dissipation process, for instance, it can be observed from the state of an atom which spontaneously decays, the state of a photon in a leaky cavity or an interferometer, and the zero-temperature energy relaxation of a superconducting qubit [19, 29].

Although Alice and Bob initially share a pure entangled state $|\Phi\rangle$, the resulting state ρ_D is not a pure state since each particle suffers from amplitude damping decoherence with strengths of D_A and D_B , respectively [7, 24]. The concurrence [30] of the final state ρ_D , C_D is given by

$$C_D = \max \left\{ 0, \Lambda_D \equiv 2\sqrt{\bar{D}_A \bar{D}_B} |\beta| (|\alpha| - \sqrt{\bar{D}_A \bar{D}_B} |\beta|) \right\}, \quad (1)$$

where $C_D = \Lambda_D$ if $\Lambda_D > 0$ and C_D is always less than the concurrence of the initial state, $2|\alpha\beta|$. From Eq. (1), it is clear that for $|\alpha| \geq |\beta|$, $C_D = 0$ only when $D_A = 1$ or $D_B = 1$, meaning that the entanglement exists except the case that the final state ρ_D is fully damped by decoherence ($D_i = 1$). On the other hand, for $|\alpha| < |\beta|$, entanglement completely disappears when $\sqrt{\bar{D}_A \bar{D}_B} > |\alpha/\beta|$, which is clearly less than the maximum level of the decoherence. Thus, ESD occurs only if $|\alpha| < |\beta|$ [7].

Let us now describe our strategy to avoid ESD as shown in Fig. 2(b). At first, Alice and Bob initially share a pure entangled state $|\Phi\rangle$. Then, Alice performs a weak measurement $W_A(p)$ on her qubit before her qubit undergoes decoherence, see Fig. 2(b). Here, weak measurement partially collapses a single qubit state towards $|0\rangle_S$. The weak measurement operator $W(p)$ can be written as $W(p) = |0\rangle\langle 0| + \sqrt{1-p}|1\rangle\langle 1|$ where p is the strength of the weak measurement [20]. Since only $|1\rangle_S$ state undergoes decoherence, the system states can partially avoid decoherence by reducing the portion of $|1\rangle_S$ state with weak measurements. Note that the initial state $|\Phi\rangle$ is transformed into $|\Phi'\rangle$ by a weak measurement and $|\Phi'\rangle$ is still a pure state.

Then each qubit undergoes separate decoherence and $|\Phi'\rangle$ evolves to a mixed state ρ' .

Alice now performs a reversing measurement $R_A(p_r)$ on her qubit as shown in Fig. 2(b). A reversing measurement is also a weak measurement but it partially collapses the state towards the opposite direction, i.e., $|1\rangle_S$. The reversing measurement operator is given as $R(p_r) = \sqrt{1-p_r}|0\rangle\langle 0| + |1\rangle\langle 1|$ where p_r is the strength of the reversing measurement. The reversing strength we used is $p_r = p + D_A\bar{p}$ where $\bar{p} \equiv 1 - p$ [21]. Here, Bob does not play any role in the whole procedure. Note that the scheme also works well if only Bob carries out single-qubit quantum measurement reversal on his qubit, i.e., $W_B(p)$ and $R_B(p_r)$. Note that the strength of the reversing measurement which Bob performs on his qubit is $p_r = p + D_B\bar{p}$.

After Alice alone performs the single-qubit quantum measurement reversal on her qubit, the concurrence of the two-qubit state ρ_A , C_A , can be evaluated by

$$C_A = \max \left\{ 0, \Lambda_A = \frac{2\sqrt{D_B}|\beta|(|\alpha| - \sqrt{D_A D_B \bar{p}}|\beta|)}{1 + D_A \bar{p} |\beta|^2} \right\}, \quad (2)$$

where $C_A = \Lambda_A$ if $\Lambda_A > 0$, otherwise $C_A = 0$. Note that $C_A > C_D$, meaning that ρ_A is more entangled than ρ_D . For the case with Bob's single-qubit quantum measurement reversal, C_B is the same as C_A except the fact that D_A and D_B are interchanged, and C_A and C_B give the same value when $D_A = D_B = D$.

From Eq. (2), we can find several remarkable results. First of all, Λ_A is monotonic increasing function of p , meaning that the resulting state ρ_A becomes more entangled as the weak and reversing strengths increase. Note that the concurrence of the initial state $|\Phi\rangle$, $2|\alpha\beta|$, cannot be fully retrieved since only Alice performs single-qubit quantum measurement reversal on her qubit. However, even in the ESD condition, ρ_A can have non-zero entanglement if the strengths of the weak and its corresponding reversing measurements ($p_r = p + D_A\bar{p}$) are larger than the threshold value, i.e., $p \geq 1 - |\alpha/\beta|^2 / (D_A D_B)$. Hence, we can conclude that Alice can avoid ESD by performing single-qubit quantum measurement reversal only on her qubit without Bob's help. Once Alice and Bob share non-zero entanglement against decoherence, they can prepare a maximally entangled state from multiple copies of less entangled states using entanglement distillation protocols [25–28].

3. Experiment

The experimental setup for demonstrating that Alice or Bob alone can avoid ESD and prevent complete loss of entanglement against decoherence using single-qubit quantum measurement reversal is shown in Fig. 3. Two-qubit entangled states are prepared by two-photon polarization states which are generated via spontaneous parametric down conversion process. A 6 mm type-I β -BaB₂O₄ crystal is pumped by a 405 nm diode laser beam (100 mW) and a pair of down-converted photons centered at 810 nm are generated on the frequency-degenerate, non-collinear phase matching condition. Each down-converted photon is frequency-filtered using an interference filter with full width at half-maximum bandwidth of 5 nm. Then, the two-qubit entangled state $|\Phi\rangle = \alpha|00\rangle + \beta|11\rangle$ can be prepared using quantum interferometry [31] and glass-plates oriented at Brewster angle (BPs) [20]. Here, $|0\rangle$ and $|1\rangle$ correspond to the horizontally ($|H\rangle$) and vertically ($|V\rangle$) polarized photons, respectively.

The weak measurement on the polarization qubit can be implemented using BPs since BP transmits horizontally polarized photons without any reflection while reflecting vertically polarized photons with some probability [20]. The reversing measurement partially collapses the state to the opposite direction, so it can be realized by adding 45° half-wave plates (HWPs) for bit-flip operations before and after BPs. The strengths of weak and reversing measurement p and p_r can be increased by adding more BPs. The amplitude damping decoherence for the photonic system can be realized using a displaced Sagnac interferometer [7, 22, 24]. In experiment,

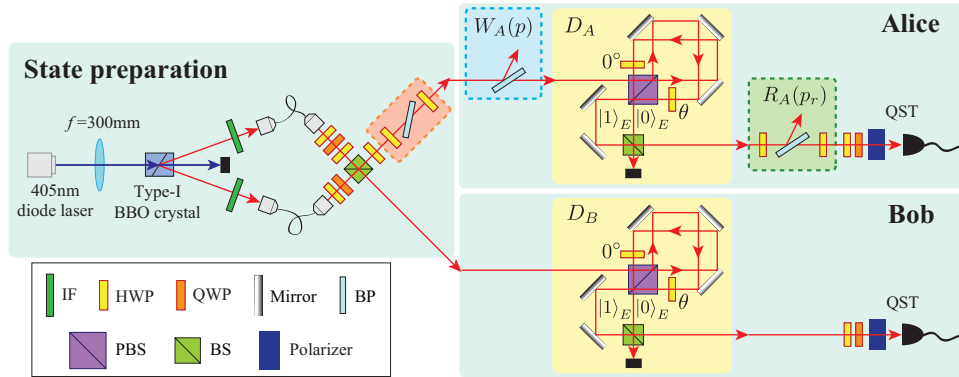


Fig. 3. Experimental setup. A set of BPs and HWPs at the state preparation part is exploited for preparing the non-maximal entangled states. Weak and reversing measurements are also implemented by BPs and 45° HWPs. The amplitude damping channel for single qubit polarization state is realized using displaced Sagnac-type interferometer and additional beam splitters [7, 22, 24]. IF: interference filter, HWP: half-wave plate, QWP: quarter-wave plate, BP: Brewster-angle glass plate, PBS: polarizing beam splitter, BS: beam splitter, QST: quantum state tomography.

the system qubit is encoded in the polarization of the single photon ($|H\rangle = |0\rangle_S$, $|V\rangle = |1\rangle_S$) and the environment qubit is encoded in the path of the single photon, $|0\rangle_E$ and $|1\rangle_E$, see Fig. 3. Finally, the resulting states are analyzed by quantum state tomography.

4. Results and analysis

Before confirming whether our scheme works well, we have investigated how the initial entangled state $|\Phi\rangle = \alpha|00\rangle + \beta|11\rangle$ is affected by the identical decoherence ($D_A = D_B = D$). We evaluated the concurrence of the final state ρ_D from the density matrices which are experimentally reconstructed by the quantum state tomography. For the two entangled input states with $|\alpha| = |\beta|$ and $|\alpha| = 0.481 < |\beta|$, we measured C_D (Λ_D) as increasing the strength of the decoherence D and the results are shown in Fig. 4(a). As expected, C_D decreases as D increases in both cases. Note that ESD is observed for the case of $|\alpha| = 0.481$.

Then, consider the case that only Alice or Bob alone carries out single-qubit quantum measurement reversal to avoid complete loss of entanglement when each qubit undergoes separate decoherence. We performed the experiment for the identical damping case, i.e., $D_A = D_B = D$. In addition, to simulate the situation in which ESD can take place, we chose $D = 0.617 \pm 0.017$. Figure 4(b) shows the experimental results for C_A and C_B (Λ_A and Λ_B) as a function of p for two initial entangled states. We have collected experimental data up to $p = 0.617$ due to low success probabilities associated with weak and reversing measurements for larger p . As expected from Eq. (2), C_A and C_B become larger as p increases. In addition, for the input state with $|\alpha| = 0.481$ which experiences ESD without introducing quantum measurement reversal, C_A and C_B can have non-zero values when strengths of the weak and reversing measurements are larger than the threshold value. This result demonstrates that Alice and Bob can share non-zero entanglement even in the ESD condition using only single-qubit quantum measurement reversal, i.e., ESD can be avoided by Alice or Bob alone.

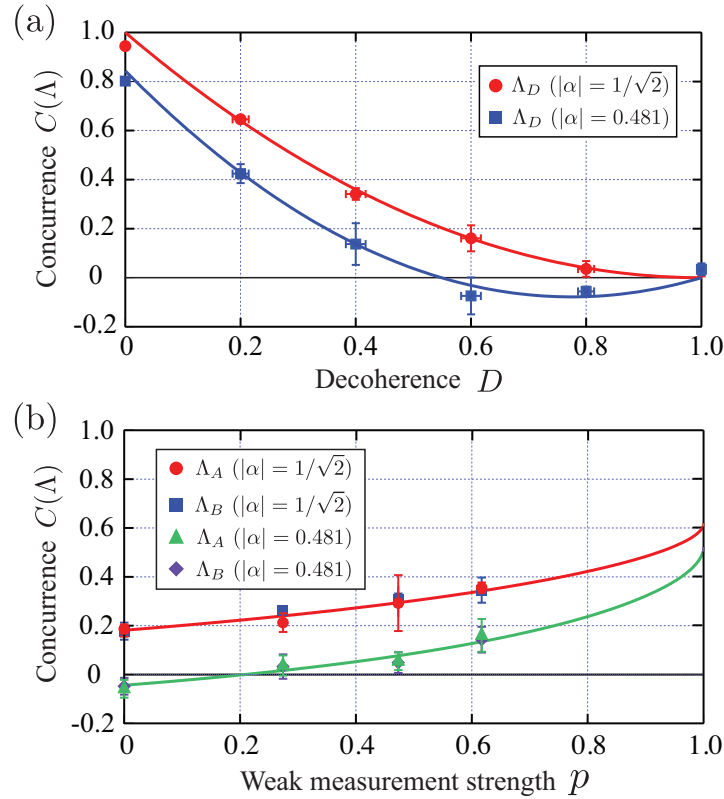


Fig. 4. (a) Concurrence C_D of the resulting state ρ_D decreases as the strength of the decoherence (D) increases. (b) Concurrence C_A (C_B) of the final state ρ_A (ρ_B) in the case that only Alice (Bob) performs single-qubit quantum measurement reversal on her (his) qubit ($D_A = D_B = 0.617$). p is the strength of the weak measurement. Solid lines are theoretical results. Negative values corresponds to Λ_D for (a), and Λ_A and Λ_B for (b), respectively. Note that $C = 0$ when $\Lambda < 0$ since $C = \max\{0, \Lambda\}$. We evaluated the fidelity between the ideally expected state and the experimentally reconstructed state for ρ_A and ρ_B . The fidelity values for ρ_A (F_A) and ρ_B (F_B) are averaged from the experimental data of (b), and we obtain $F_A = 0.945 \pm 0.024$ and $F_B = 0.935 \pm 0.028$.

5. Conclusion

When two entangled qubits, each owned by Alice and Bob, experience separate decoherence, the amount of entanglement decreases and sometimes ESD occurs. We have demonstrated that Alice or Bob alone overcomes ESD and still share non-zero entanglement after decoherence with quantum measurement reversal on only one of the two entangled qubits. Since any small amount of entanglement shared by Alice and Bob can be concentrated, we believe that our scheme has important applications in quantum information protocols based on distributed or stored entangled qubits as they are subject to decoherence. Moreover, our scheme can be directly applied to other qubit systems experiencing decoherence, such as, two-level atoms with spontaneous decay, superconducting qubits with zero-temperature energy relaxation, and so on.

Appendix : Reversing measurement strength under decoherence

When an initial quantum state $|\psi_{\text{in}}\rangle = \alpha|0\rangle + \beta|1\rangle$ does not suffer any decoherence ($D = 0$), the reversing measurement for the weak measurement $W(p) = |0\rangle\langle 0| + \sqrt{1-p}|1\rangle\langle 1|$ is $R(p_r) = \sqrt{1-p_r}|0\rangle\langle 0| + |1\rangle\langle 1|$ with $p_r = p$ [17]. The quantum state $|\psi_{\text{in}}\rangle = \alpha|0\rangle + \beta|1\rangle$ is retrieved without errors only when $p_r = p$, and, thus, $p_r = p$ is the optimal reversing measurement strength for $D = 0$. Note that the optimal p_r is independent on α in this case.

However, when decoherence is introduced, $p_r = p$ is not the optimal measurement anymore and the ‘‘optimality’’ of the reversing measurement strength becomes highly non-trivial. In general, p_r is dependent on several parameters such as D , p , and α . Since the initial state cannot be retrieved perfectly, the optimal p_r value is different for maximizing, e.g., the state fidelity, the success probability, the concurrence, etc. Moreover, the optimal p_r value is also dependent on the condition of the decoherence suppression scenarios. In this section, we investigate several reversing measurement strategies and compare them with respect to the state fidelity and the success probability. Here, we consider three different situations i) a single qubit state suffers decoherence [21, 22], ii) both subsystems of the two-qubit entangled state suffer from decoherence (the scenarios considered in [24] and in this manuscript), and iii) one subsystem of the two-qubit entangled state suffers from decoherence.

A1. Single qubit case

As shown in Fig. 1(a), if a set of weak measurement $W(p)$ and reversing measurement $R(p_r)$ measurements are performed before and after decoherence (D), an initial qubit state $|\psi_{\text{in}}\rangle = \alpha|0\rangle + \beta|1\rangle$, where $|\alpha|^2 + |\beta|^2 = 1$, is transformed to the final state ρ_{out} , given as

$$\rho_{\text{out}} = \frac{1}{P_S} \begin{pmatrix} \bar{p}_r (|\alpha|^2 + D\bar{p}|\beta|^2) & \sqrt{\bar{p}_r \bar{D} \bar{p}} \alpha \beta^* \\ \sqrt{\bar{p}_r \bar{D} \bar{p}} \alpha^* \beta & \bar{D} \bar{p} |\beta|^2 \end{pmatrix}, \quad (3)$$

where $\bar{D} \equiv 1 - D$, $\bar{p} \equiv 1 - p$, $\bar{p}_r \equiv 1 - p_r$. The success probability or channel transmittance is $P_S = \bar{p}_r (|\alpha|^2 + D\bar{p}|\beta|^2) + \bar{D} \bar{p} |\beta|^2$ [21, 22].

One way to quantify performance of the decoherence suppression scheme is evaluating the state fidelity between the initial state $\rho_{\text{in}} = |\psi_{\text{in}}\rangle\langle \psi_{\text{in}}|$ and the final state ρ_{out} , i.e., $F = \langle \psi_{\text{in}} | \rho_{\text{out}} | \psi_{\text{in}} \rangle$, which is calculated to be

$$F = \frac{1 - p|\beta|^4 - p_r|\alpha|^4 - D\bar{p}|\beta|^2 [1 + (p_r - 2)|\alpha|^2] - 2|\alpha|^2|\beta|^2 [1 - \sqrt{\bar{p}_r \bar{D} \bar{p}}]}{1 - Dp_r - \bar{D} \bar{p}_r |\alpha|^2 - p(1 - Dp_r) |\beta|^2}. \quad (4)$$

Then, the reversing measurement strength p_r^{max} value which gives the maximum fidelity value F_{max} is

$$p_r^{\text{max}} = -\frac{1-p|\beta|^2}{D\bar{p}|\beta|^2 + |\alpha|^2} + \frac{(D\bar{p}+p)(|\alpha|^2 - |\beta|^2)^2 + 4|\alpha|^2 - 1 + \bar{D}\bar{p}(|\alpha|^2 - |\beta|^2) \sqrt{\frac{D\bar{p}|\beta|^2(|\alpha|^2 - |\beta|^2)^2 + |\alpha|^2}{D\bar{p}|\beta|^2 + |\alpha|^2}}}{2|\alpha|^4}. \quad (5)$$

Note that p_r^{max} depends on α , D , and p .

However, in practical decoherence scenario, we may assume that we know the magnitude of decoherence D while we do not have any prior information about the initial state $|\psi_{\text{in}}\rangle$, i.e., α is an unknown parameter [22, 24]. We consider two different state independent p_r values. First, we obtain p_r by substituting $|\alpha| = 1/\sqrt{2}$ into Eq. (5),

$$p_r^{\text{fix}} = \frac{2D + p - 2Dp}{D + 1 - Dp}, \quad (6)$$

where p_r^{fix} is now state-independent, meaning that p_r^{fix} is not a function of α .

Second, we choose p_r to be $p_r^{\text{exp}} = p + (1 - p)D$ which is used in our paper [21, 22]. The reasons we chose p_r^{exp} are the following: i) p_r^{exp} is state independent, i.e., p_r^{exp} is not a function of α and ii) the state fidelity F asymptotically approaches to 1 as the weak measurement strength $p \rightarrow 1$ regardless of α .

We now compare the state fidelity values F between the initial and final states for two different reversing measurement strength p_r^{fix} and p_r^{exp} . The state fidelity values for the strength of the reversing measurement p_r^{fix} and p_r^{exp} , respectively, are calculated to be

$$F^{\text{fix}} = \frac{1 + |\beta|^2 D \bar{p} - 2|\alpha\beta|^2 (1 - \sqrt{1 + D\bar{p}})}{1 + 2D\bar{p}|\beta|^2}, \quad (7)$$

and

$$F^{\text{exp}} = \frac{1 + D\bar{p}|\alpha\beta|^2}{1 + D\bar{p}|\beta|^2}. \quad (8)$$

F^{max} can be obtained by substituting p_r^{max} to Eq. (3). Note that F^{max} is always higher than both of F^{fix} and F^{exp} regardless of $|\alpha|$, D , and p . However, to achieve F^{max} , we need to know prior information about the initial state, meaning that the decoherence suppression scheme becomes state dependent. Thus, here, we focus on comparing F^{exp} with F^{fix} .

The numerical results for the state fidelities for reversing strengths p_r^{fix} and p_r^{exp} when $D = 0.617$ are shown in Fig. 5(a). Note that $F^{\text{exp}} > F^{\text{fix}}$ when $|\alpha|$ is larger than $|\beta|$. Since our decoherence suppression scheme exploits weak measurement, the success probability of the scheme is not unity. Hence, the success probability is also an important parameter for quantifying the performance of the scheme. The success probabilities for p_r^{fix} and p_r^{exp} , respectively,

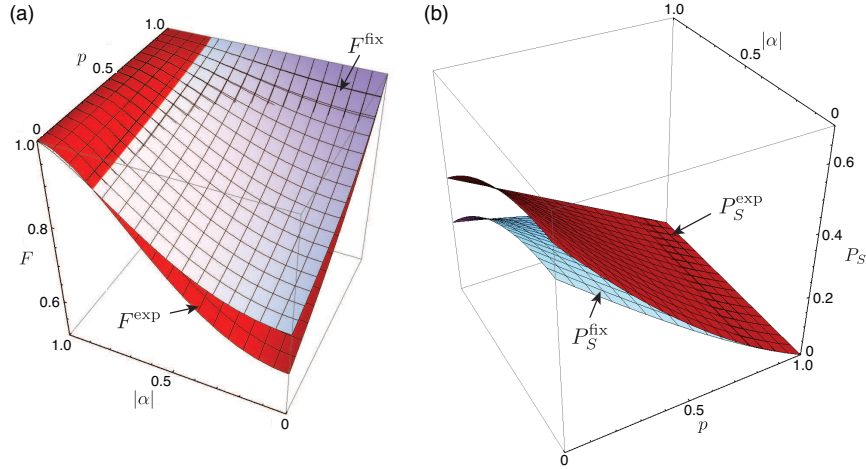


Fig. 5. Result of the scenario in Fig. 1(a) with $D = 0.617$. (a) State fidelities F^{fix} and F^{exp} as functions of $|\alpha|$ and p . F^{fix} and F^{exp} increase as the weak measurement strength p increases. (b) Success probabilities P_S^{fix} and P_S^{exp} as functions of $|\alpha|$ and p . P_S^{exp} is always larger than P_S^{fix} regardless of $|\alpha|$ and p values. Note that $F \rightarrow 1$ and $P_S \rightarrow 0$ as $p \rightarrow 1$ for both cases of p_r^{fix} and p_r^{exp} .

are given by

$$P_S^{\text{fix}} = \frac{\bar{D}\bar{p}(1+2D\bar{p}|\beta|^2)}{1+D\bar{p}} \quad \text{and} \quad P_S^{\text{exp}} = \bar{D}\bar{p}(1+D\bar{p}|\beta|^2). \quad (9)$$

P_S^{max} can be obtained by substituting p_r^{max} into P_S of Eq. (3). Note that, in most cases, P_S^{max} is lower than P_S^{fix} and P_S^{exp} since p_r^{max} is chosen for maximizing the state fidelity F .

Figure 5(b) represents the success probability dependencies on $|\alpha|$ and p for different reversing measurement strengths when $D = 0.617$. As shown in Fig. 5(b), $P_S^{\text{exp}} > P_S^{\text{fix}}$ for all values of $|\alpha|$ and p . In the single qubit case, the reversing measurement strength $p_r^{\text{exp}} = p + (1-p)D$ is more efficient than p_r^{max} and p_r^{fix} in terms of the success probability.

A2. Two-qubit case: Both subsystems suffer from decoherence and two pairs of weak and reversing measurements are performed

We consider the situation shown in Fig. 1(b) in which the initial two-qubit entangled state $|\Phi\rangle = \alpha|00\rangle + \beta|11\rangle$, where $|\alpha|^2 + |\beta|^2 = 1$, suffers from separate decoherence and two pairs of weak and reversing measurements are applied to suppress decoherence [24]. To simplify the situation, we assume that each subsystem undergoes the same magnitude of decoherence ($D_A = D_B = D$) and the strengths of weak measurements $W_A(p)$ and $W_B(p)$, and reversing measurements $R_A(p_r)$ and $R_B(p_r)$ performed on each subsystem are the same. Then, the output state ρ_{out} is given as

$$\rho_{\text{out}} = \frac{1}{P_S} \begin{pmatrix} (|\alpha|^2 + D^2|\beta|^2\bar{p}^2)\bar{p}_r^2 & 0 & 0 & \bar{p}\bar{D}\bar{p}_r\alpha\beta^* \\ 0 & D|\beta|^2\bar{D}\bar{p}^2\bar{p}_r & 0 & 0 \\ 0 & 0 & D|\beta|^2\bar{D}\bar{p}^2\bar{p}_r & 0 \\ \bar{p}\bar{D}\bar{p}_r\alpha^*\beta & 0 & 0 & |\beta|^2\bar{D}^2\bar{p}^2 \end{pmatrix}, \quad (10)$$

where $P_S = p_r\bar{D}(|\alpha|^2(Dp_r + p_r - 2) + (Dp_r - 1)^2(1 - p^2|\beta|^2 + 2p|\beta|^2))$ is the success probability. The state fidelity between the initial state and the output state is obtained to be

$$F = \frac{|\beta|^2 D^2 \bar{p}^2 [|\alpha|^2 (p_r - 2) p_r + 1] - 2 |\beta|^2 D \bar{p} [\bar{p} + |\alpha|^2 (p - p_r)] + [\bar{p} + |\alpha|^2 (p - p_r)]^2}{|\alpha|^2 \bar{D} p_r [(D + 1) p_r - 2] + [|\beta|^2 (p - 2) p + 1] (D p_r - 1)^2}, \quad (11)$$

and the reversing measurement strength maximizing F is

$$p_r^{\text{max}} = \frac{\bar{D}\bar{p} + 2p|\alpha|^2}{2|\alpha|^2(1 - D\bar{p})} - \frac{\bar{D}\bar{p}\sqrt{\frac{|\alpha|^2 - D\bar{p}|\beta|^2(4|\alpha|^2 - D\bar{p})}{|\alpha|^2 + D^2\bar{p}^2|\beta|^2}}}{2|\alpha|^2(1 - D\bar{p})}, \quad (12)$$

if i) $|\alpha| \geq \frac{1}{\sqrt{2}}$ or ii) $|\alpha| < \frac{1}{\sqrt{2}}$ and $D\bar{p}|\beta|^2 < |\alpha|^2 < \bar{p}|\beta|^2$. Otherwise, $p_r = 1$ maximizes F , meaning that the reversing measurement p_r should be projection measurement regardless of the weak measurement strength p .

As we did in the single qubit case, p_r^{fix} is obtained by substituting $\alpha = 1/\sqrt{2}$ into Eq. (12) and we obtain

$$p_r^{\text{fix}} = \frac{\sqrt{D^2\bar{p}^2 + 1} - \bar{D}\bar{p}}{\sqrt{D^2\bar{p}^2 + 1}}, \quad (13)$$

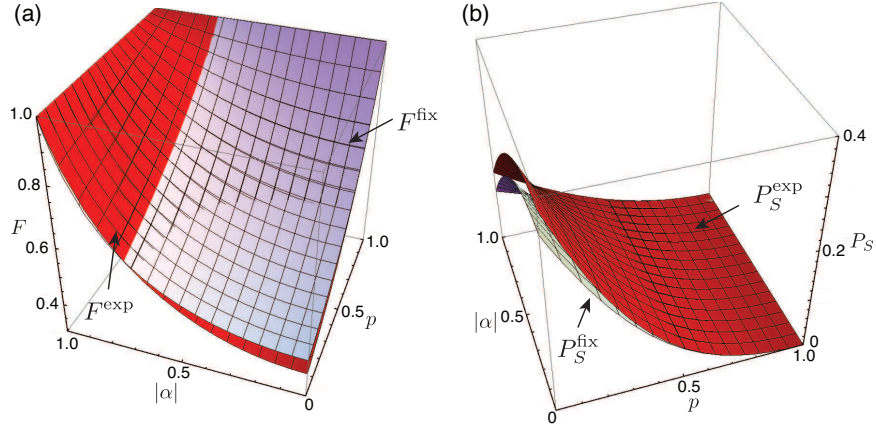


Fig. 6. Result of the scenario in Fig. 1(b) with $D_A = D_B = 0.617$. (a) State fidelities F^{fix} and F^{exp} as functions of $|\alpha|$ and p . The state fidelities increase as the weak measurement strength p increases. (b) Success probabilities P_S^{fix} and P_S^{exp} as functions of $|\alpha|$ and p . Note that $P_S \rightarrow 0$ as $p \rightarrow 1$ for all both cases.

and the corresponding state fidelity F^{fix} for p_r^{fix} is given as

$$F^{\text{fix}} = \frac{2|\alpha|^2|\beta|^2(\sqrt{D^2\bar{p}^2+1}-1) + D^2\bar{p}^2|\beta|^2 + 1}{2D\bar{p}|\beta|^2(\sqrt{D^2\bar{p}^2+1} + D\bar{p}) + 1}. \quad (14)$$

On the other hand, the state fidelity F^{exp} for $p_r^{\text{exp}} = p + (1-p)D$ is calculated to be

$$F^{\text{exp}} = \frac{1 + D^2\bar{p}^2|\alpha|^2|\beta|^2}{1 + D\bar{p}|\beta|^2(D\bar{p} + 2)}. \quad (15)$$

The numerical results for the state fidelities F for p_r^{fix} and p_r^{exp} are shown in Fig. 6(a). As shown in Fig. 6(a), the general tendency of F^{fix} and F^{exp} are similar to the results of the single qubit case, see Fig. 5(a). F^{exp} is generally larger than F^{fix} when $|\alpha|$ is larger than $|\beta|$.

Finally, the success probabilities for p_r^{fix} and p_r^{exp} , respectively, are calculated to be

$$P_S^{\text{fix}} = \bar{D}^2\bar{p}^2 \left(\frac{D^2\bar{p}^2|\beta|^2 + |\alpha|^2}{D^2\bar{p}^2 + 1} + \frac{2D\bar{p}|\beta|^2}{\sqrt{D^2\bar{p}^2 + 1}} + |\beta|^2 \right), \quad (16)$$

and

$$P_S^{\text{exp}} = \bar{D}^2\bar{p}^2 \left[1 + D\bar{p}|\beta|^2(D\bar{p} + 2) \right]. \quad (17)$$

Figure 6(b) shows the success probabilities P_S for various reversing measurement strength p_r . As shown in Fig. 6(b), P_S^{exp} is always larger than P_S^{fix} in any combination of $|\alpha|$ and p . The general tendency of the success probabilities are similar to the single qubit case in that P_S^{exp} is larger than P_S^{fix} .

A3. Two-qubit case: Both subsystems suffer from decoherence and one pair of weak and reversing measurements are performed

In this section, we consider the scenario of this paper, see Fig. 1(c). Each subsystem of the initial entangled state $|\Phi\rangle = \alpha|00\rangle + \beta|11\rangle$, where $|\alpha|^2 + |\beta|^2 = 1$, undergoes separate decoherence

and a set of weak measurement $W_A(p)$ and reversing measurement $R_A(p_r)$ is performed only on the subsystem undergoing decoherence (A). If we assume each subsystem undergoes the identical decoherence ($D_A = D_B = D$), the output state ρ_{out} is given as

$$\rho_{\text{out}} = \frac{1}{P_S} \begin{pmatrix} \bar{p}_r (D^2 \bar{p} |\beta|^2 + |\alpha|^2) & 0 & 0 & \alpha \beta^* \bar{D} \sqrt{\bar{p}} \sqrt{\bar{p}_r} \\ 0 & D \bar{D} \bar{p} |\beta|^2 \bar{p}_r & 0 & 0 \\ 0 & 0 & D \bar{D} \bar{p} |\beta|^2 & 0 \\ \alpha^* \beta \bar{D} \sqrt{\bar{p}} \sqrt{\bar{p}_r} & 0 & 0 & \bar{D}^2 \bar{p} |\beta|^2 \end{pmatrix}, \quad (18)$$

where $P_S = |\alpha|^2 [p - p_r (\bar{D} + Dp)] + \bar{p} (1 - Dp_r)$ and the corresponding state fidelity between the initial state and the final state is calculated to be

$$F = \frac{D^2 \bar{p} |\beta|^2 (1 - |\alpha|^2 p_r) - 2 |\alpha|^2 (\sqrt{\bar{p} \bar{p}_r} - 1) (D |\beta|^2 - 1) - |\alpha|^4 (2 \sqrt{\bar{p} \bar{p}_r} + p_r - 2) - 2D |\beta|^2 + (2D - 1)p |\beta|^4 + 1}{(p |\beta|^2 - 1)(D p_r - 1) - \bar{D} |\alpha|^2 p_r}. \quad (19)$$

Since the reversing measurement strength p_r^{max} which maximizes F is rather complicated and cannot be simplified, we provide p_r^{fix} instead of p_r^{max} . p_r^{fix} is calculated to be

$$p_r^{\text{fix}} = \frac{(2D\bar{p} + p) \left[2 - D\bar{p} \left(D(2D\bar{p} + p) + \sqrt{D \left[D \left((2D\bar{p} + p)^2 - 4\bar{p} \right) - 4p \right] + 4 - 2} \right) \right]}{2(D\bar{p} + 1)^2}. \quad (20)$$

Since the final expressions of F^{fix} and P_S^{fix} are also complicated, we omit their analytic expressions. F^{exp} and P_S^{exp} values for p_r^{exp} , respectively, are given as

$$F^{\text{exp}} = \frac{D^2 \bar{p} |\alpha|^2 |\beta|^2 + 2 (\sqrt{\bar{D}} - 1) |\alpha|^2 |\beta|^2 - D |\beta|^4 + 1}{D \bar{p} |\beta|^2 + 1}, \quad (21)$$

and

$$P_S^{\text{exp}} = \bar{D} \bar{p} (D \bar{p} |\beta|^2 + 1). \quad (22)$$

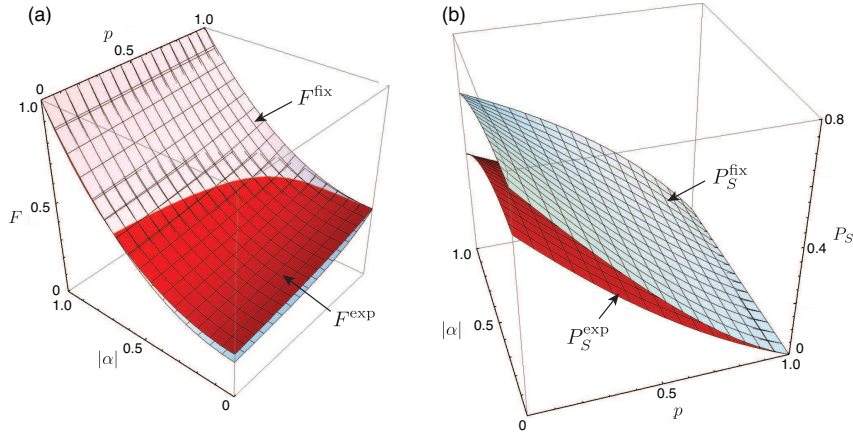


Fig. 7. Result of the scenario in Fig. 1(c) with $D_A = D_B = 0.617$. (a) State fidelities F^{fix} and F^{exp} as functions of $|\alpha|$ and p . The state fidelities increase as the weak measurement strength p increases. (b) Success probabilities P_S^{fix} and P_S^{exp} as functions of $|\alpha|$ and p . P_S^{fix} is always larger than P_S^{exp} regardless of $|\alpha|$ and p values. Note that F does not approach to unity and $P_S \rightarrow 0$ as $p \rightarrow 1$ for both cases of p_r^{fix} and p_r^{exp} .

Although we do not provide explicit forms of F^{fix} and P_S^{fix} due to their complexity, we show numerical results to compare F^{fix} and P_S^{fix} with F^{exp} and P_S^{exp} , respectively. Figure 7(a) shows the state fidelity results for various reversing strengths. Since a single pair of weak and reversing measurements cannot suppress two independent decoherence, the state fidelities F cannot achieve unity even in the case that $p \rightarrow 1$. Note that $F \rightarrow 1$ as $p \rightarrow 1$ in both of Fig. 5(a) and Fig. 6(b). Another thing to note is that F^{fix} is larger than F^{exp} when $|\alpha|$ is larger than $|\beta|$ in Fig. 7(a) while F^{exp} is larger than F^{fix} when $|\alpha|$ is larger than $|\beta|$ in both of Fig. 5(a) and Fig. 6(a). Interestingly, the difference between F^{fix} , and F^{exp} is very small in any combination of $|\alpha|$ and p in Fig. 7(a).

The general tendency of the success probabilities in this case are opposite to the previous cases, see Fig. 7(b). P_S^{fix} is always larger than P_S^{exp} in Fig. 7(b); however, P_S^{exp} is always larger than P_S^{fix} in both of Fig. 5(b) and Fig. 6(b).

A4. Two-qubit case: One subsystem suffers from decoherence and one pair of weak and reversing measurements are performed

Finally, we consider the case of Fig. 1(c) with $D_A = D$ and $D_B = 0$. Here only the subsystem A of the initial entangled state $|\Phi\rangle = \alpha|00\rangle + \beta|11\rangle$, where $|\alpha|^2 + |\beta|^2 = 1$, suffers from decoherence and a set of weak measurement $W_A(p)$ and reversing measurement $R_A(p_r)$ is performed on the subsystem A. Then, the output state ρ_{out} becomes

$$\rho_{\text{out}} = \frac{1}{P_S} \begin{pmatrix} |\alpha|^2 \bar{p}_r & 0 & 0 & \sqrt{\bar{D}}\sqrt{\bar{p}}\sqrt{\bar{p}_r}\alpha\beta^* \\ 0 & D|\beta|^2 \bar{p}\bar{p}_r & 0 & 0 \\ 0 & 0 & 0 & 0 \\ \sqrt{\bar{D}}\sqrt{\bar{p}}\sqrt{\bar{p}_r}\alpha^*\beta & 0 & 0 & |\beta|^2 \bar{D}\bar{p} \end{pmatrix}, \quad (23)$$

where $P_S = |\beta|^2 \bar{D}\bar{p} + |\beta|^2 D\bar{p}\bar{p}_r + |\alpha|^2 \bar{p}_r$ and the state fidelity between the input state and the output state is given as

$$F = \frac{D\bar{p}|\beta|^4 + |\alpha|^4 (2\sqrt{\bar{D}\bar{p}\bar{p}_r} + p_r - 2) - 2|\alpha|^2 (\sqrt{\bar{D}\bar{p}\bar{p}_r} - 1) + p|\beta|^4 - 1}{\bar{D}|\alpha|^2 p_r + (p|\beta|^2 - 1)(1 - Dp_r)}, \quad (24)$$

and the reversing measurement strength p_r^{max} that maximizes F is

$$p_r^{\text{max}} = \frac{D^2 \bar{p}^2 |\beta|^4 - D\bar{p}|\alpha|^2 (|\beta|^2 + 1) + p|\alpha|^4}{(|\alpha|^2 - D\bar{p}|\beta|^2)^2}. \quad (25)$$

Then, p_r^{fix} is evaluated by substituting $\alpha = 1/\sqrt{2}$ into Eq. (25) and p_r^{fix} is given as

$$p_r^{\text{fix}} = \frac{D^2 \bar{p}^2 - 3D\bar{p} + p}{(D\bar{p} - 1)^2}. \quad (26)$$

The state fidelity values for p_r^{fix} and p_r^{exp} , respectively, are given as

$$F^{\text{fix}} = \frac{(D\bar{p}|\beta|^2 + 1)^2}{D\bar{p}|\beta|^2 (D\bar{p} + 3) + 1}, \quad \text{and} \quad F^{\text{exp}} = \frac{1}{D\bar{p}|\beta|^2 + 1}. \quad (27)$$

The success probabilities for p_r^{fix} and p_r^{exp} , respectively, are given as

$$P_S^{\text{fix}} = \frac{\bar{D}\bar{p} [D\bar{p}|\beta|^2 (D\bar{p} + 3) + 1]}{(D\bar{p} + 1)^2}, \quad \text{and} \quad P_S^{\text{exp}} = \bar{D}\bar{p} (D\bar{p}|\beta|^2 + 1). \quad (28)$$

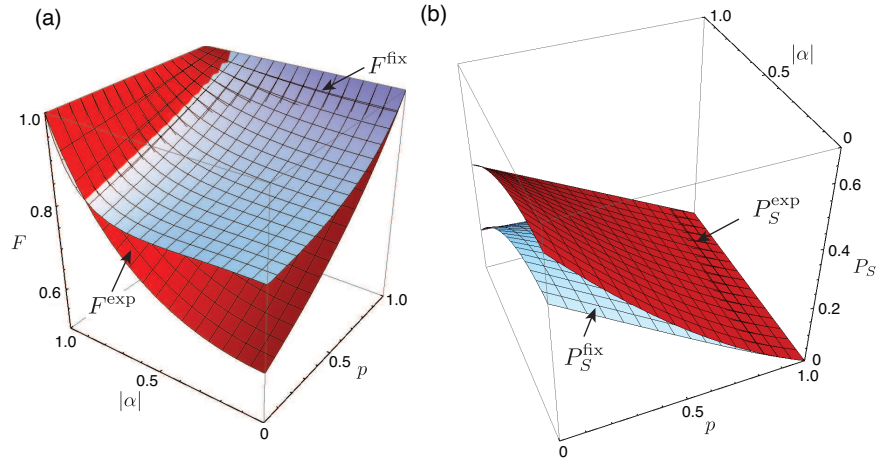


Fig. 8. Result of the scenario in Fig. 1(c) with $D_A = 0.617$ and $D_B = 0$. (a) State fidelities F^{fix} and F^{exp} as functions of $|\alpha|$ and p . (b) Success probabilities P_S^{fix} and P_S^{exp} as functions of $|\alpha|$ and p . P_S^{exp} is always larger than P_S^{fix} regardless of $|\alpha|$ and p values. Note that $F \rightarrow 1$ and $P_S \rightarrow 0$ as $p \rightarrow 1$ for both cases of p_r^{fix} and p_r^{exp} .

The numerical results for the state fidelities and the success probabilities for various reversing measurement strengths are shown in Fig. 8. In this scheme, the general tendencies of the state fidelities and the success probabilities are similar to the single qubit case shown in Fig. 5, i.e., $F^{\text{exp}} > F^{\text{fix}}$ when $|\alpha|$ is larger than $|\beta|$ and $P_S^{\text{exp}} > P_S^{\text{fix}}$ regardless of $|\alpha|$ and p .

A5. Conclusion

In conclusion, we have investigated the state fidelities F and the success probabilities P_S for various decoherence suppression schemes. Our results suggest that there is no reversing measurement which maximizes the state fidelity and the success probability simultaneously. In many cases, a trade-off relation between F and P_S holds, in other words, the higher the state fidelity, the lower the success probability, vice versa. Therefore, one should choose a proper p_r value for a specific application, after carefully considering the trade-off relation.

Acknowledgments

This work was supported in part by the National Research Foundation of Korea (Grant No. 2013R1A2A1A01006029 and 2011-0021452). H.-T.L. and J.-C.L. acknowledge support from the National Junior Research Fellowship (Grant No. 2012-000642 and 2012-000741, respectively).